Chapter 7
The Activity-Based Theoretical K–Mg and Na–Mg Geoindicators

Abstract Assuming that geothermal reservoir liquids are in equilibrium with clinochlore, muscovite, adularia, albite, and a silica mineral (Giggenbach, 1988), their K^2/Mg- and Na^2/Mg-activity ratios are controlled by the aquifer temperature, T, the order-disorder degree of hydrothermal adularia, Z, and the mineral activity product, MAP, involving the activity of clinochlore in hydrothermal chlorite and the activity of muscovite in hydrothermal illite. Knowing Z and T, it is possible to obtain MAP. For the reservoir liquids with negative MAP values, the K^2/Mg- and Na^2/Mg-activity ratios can be used to calculate the minimum activities of clinochlore in chlorites and of muscovite in illites, which have limited importance for practical purposes. For the reservoir liquids with positive MAP values, the K^2/Mg- and Na^2/Mg-activity ratios can be utilized to compute the minimum concentrations of excess (non-equilibrium) Mg and, consequently, to identify and quantify the processes controlling excess Mg, such as cooling and mixing, which may lead to Mg-silicate (e.g., smectite) scaling. This is probably the most valuable information provided by the activity-based theoretical K-Mg and Na-Mg geoindicators. The K-Mg and Na-Mg exchange reactions involving other Mg-minerals are not explored to develop other K-Mg and Na-Mg geoindicators due to the restricted temperature intervals in which they are expected to be effective and the limitations caused by the varying characteristics of the relevant Mg-bearing minerals.

As already discussed in Sect. 5.6, Giggenbach (1988) assumed that (i) the K–Mg geothermometer is controlled by coexistence, at equilibrium, of clinochlore (Clc), muscovite (Ms), chalcedony (Chc), and adularia (Adl), as expressed by reaction (5.141), and (ii) the Na–Mg geothermometer is governed by co-occurrence, at equilibrium, of the same hydrothermal minerals plus albite (Ab), as indicated by reaction (5.142). Although the K–Mg and Na–Mg geothermometers might be controlled by exchange reactions involving Mg-bearing solid phases other than chlorites, as discussed in Sect. 5.6.3, let us consider reactions (5.141) and (5.142), which are rewritten here reversing their direction for convenience:

R. Cioni and L. Marini, *A Thermodynamic Approach to Water Geothermometry*, Springer Geochemistry, https://doi.org/10.1007/978-3-030-54318-1_7

$$2.8KAlSi_3O_8 + Mg^{2+} + 1.6H_2O = 0.2Mg_5Al_2Si_3O_{10}(OH)_8 + 0.8KAl_3Si_3O_{10}(OH)_2 + 5.4SiO_2 + 2K^+, \tag{7.1}$$

$$0.8KAlSi_3O_8 + 2NaAlSi_3O_8 + Mg^{2+} + 1.6H_2O = 0.2Mg_5Al_2Si_3O_{10}(OH)_8 + 0.8KAl_3Si_3O_{10}(OH)_2 + 5.4SiO_2 + 2Na^+. \tag{7.2}$$

7.1 The Log K of the K–Mg and Na–Mg Exchange Reactions

The thermodynamic equilibrium constants of reactions (7.1) and (7.2) are the inverse of Eqs. (5.143) and (5.144), that is:

$$K_{K-Mg} = \frac{a_{Clc}^{0.2} \cdot a_{Ms}^{0.8} \cdot a_{Chc}^{5.4} \cdot a_{K^+}^2}{a_{Adl}^{2.8} \cdot a_{Mg^{2+}} \cdot a_{H_2O}^{1.6}} \tag{7.3}$$

$$K_{Na-Mg} = \frac{a_{Clc}^{0.2} \cdot a_{Ms}^{0.8} \cdot a_{Chc}^{5.4} \cdot a_{Na^+}^2}{a_{Adl}^{0.8} \cdot a_{Ab}^2 \cdot a_{Mg^{2+}} \cdot a_{H_2O}^{1.6}} \tag{7.4}$$

Since adularia, albite and chalcedony are usually pure or relatively pure minerals, their activities can be assumed to be equal to 1. Also the activity of water does not deviates significantly from unity, if the ionic strength of the aqueous solution is lower than ~1 mol/kg. Therefore, Eqs. (7.3) and (7.4) can be generally simplified and rearranged as follows:

$$\frac{a_{K^+}^2}{a_{Mg^{2+}}} \cong \frac{K_{K-Mg}}{a_{Clc}^{0.2} \cdot a_{Ms}^{0.8}}. \tag{7.5}$$

$$\frac{a_{Na^+}^2}{a_{Mg^{2+}}} \cong \frac{K_{Na-Mg}}{a_{Clc}^{0.2} \cdot a_{Ms}^{0.8}}. \tag{7.6}$$

Equations (7.5) and (7.6) indicate that the K^2/Mg- and Na^2/Mg-activity ratios of geothermal liquids are expected to depend not only on the equilibrium temperature but also on the mineral activity product $a_{Clc}^{0.2} \cdot a_{Ms}^{0.8}$, which is indicated by the acronym MAP in the subsequent discussion. In turn, the activities of clinochlore and muscovite depend on the crystallo-chemical characteristics of hydrothermal chlorites and illites, respectively. Therefore, it is worth to recall that:

1. The 181 hydrothermal chlorites considered in Sect. 4.4.3 have activity of the clinochlore endmember varying between 4.39×10^{-7} and 0.250, with an average of 0.0553, a median of 0.0451 and a standard deviation of 0.0484.
2. The 75 hydrothermal illites taken into account in Sect. 4.3.2 have activity of the muscovite endmember ranging between 0.007 and 0.875, with an average of 0.654, a median of 0.688 and a standard deviation of 0.156.
3. Based on the average a_{Ms} and a_{Clc} values, log MAP has a mean of −0.399 and is expected to vary from −0.674 to −0.270 considering a range of $\pm 1\sigma$ around the mean a_{Ms} and a_{Clc} values.

Further complications are posed by Al–Si order-disorder on the tetrahedral sites of adularia as discussed in Sects. 4.2.3 and 5.3.3. Therefore, an adularia with ordering parameter Z varying from 0 (i.e., high-sanidine) to 1 (i.e., maximum-microcline) at steps of 0.1 units was alternatively assumed to be involved in reactions (7.1) and (7.2).

Another point to be considered is the basal spacing of clinochlore. Based on the pertinent discussion in Sect. 4.4.4, 7Å-clinochlore was considered to take part to reactions (7.1) and (7.2)

Either the quartz/chalcedony mechanical mixture, above 175 °C, or chalcedony, below 175 °C, were assumed to participate to reactions (7.1) and (7.2), whose thermodynamic properties were calculated by means of SUPCRT92, considering the thermodynamic data of solid phases of Helgeson et al. (1978), for temperatures varying from 0 to 350 °C, at steps of 25 °C, and for values of the ordering parameter Z of adularia varying from 0 to 1, at steps of 0.1 units.

The computed log K_{K-Mg} values (Table 7.1) are a function of the absolute temperature inverse and the ordering parameter Z of adularia as defined by the following two relations:

$$\log K_{K-Mg} = \left(\frac{-1621.2}{T} + 2.0798\right) \cdot Z - \frac{105,276}{T^2} - \frac{2019.8}{T} + 5.6865 \quad (7.7)$$

$$\log K_{K-Mg} = \left(\frac{-1621.2}{T} + 2.0798\right) \cdot Z + \frac{450,637}{T^2} - \frac{4280.5}{T} + 8.4530 \quad (7.8)$$

Equation (7.7) applies from 0 to 175 °C, whereas Eq. (7.8) is valid from 175 to 325 °C.

The calculated log K_{Na-Mg} values (Table 7.2) depend on the absolute temperature inverse and the ordering parameter Z of adularia as described by the following two equations:

$$\log K_{Na-Mg} = \left(\frac{-463.264}{T} + 0.5944\right) \cdot Z + \frac{104,027}{T^2} - \frac{1646.0}{T} + 5.7524 \quad (7.9)$$

$$\log K_{Na-Mg} = \left(\frac{-462.976}{T} + 0.5938\right) \cdot Z + \frac{752,484}{T^2} - \frac{4407.2}{T} + 9.1807 \quad (7.10)$$

Table 7.1 Logarithm of the thermodynamic equilibrium constant of reaction (7.1) involving pure clinochlore, muscovite, adularia, and chalcedony (for T < 175 °C) or quartz/chalcedony (for T > 175 °C), log K_{K-Mg}, as a function of temperature and the ordering parameter Z of adularia

T(°C)	Z = 1	Z = 0.9	Z = 0.8	Z = 0.7	Z = 0.6	Z = 0.5	Z = 0.4	Z = 0.3	Z = 0.2	Z = 0.1	Z = 0
0.01	−6.9744	−6.5888	−6.2033	−5.8178	−5.4322	−5.0467	−4.6612	−4.2757	−3.8901	−3.5046	−3.1191
25	−5.6303	−5.2946	−4.9588	−4.6230	−4.2872	−3.9514	−3.6157	−3.2799	−2.9441	−2.6083	−2.2726
50	−4.5075	−4.2138	−3.9200	−3.6263	−3.3326	−3.0389	−2.7452	−2.4515	−2.1578	−1.8641	−1.5704
75	−3.5590	−3.3013	−3.0437	−2.7860	−2.5283	−2.2707	−2.0130	−1.7553	−1.4976	−1.2400	−0.9823
100	−2.7477	−2.5213	−2.2948	−2.0683	−1.8419	−1.6154	−1.3889	−1.1624	−0.9360	−0.7095	−0.4830
125	−2.0447	−1.8455	−1.6463	−1.4472	−1.2480	−1.0488	−0.8496	−0.6504	−0.4512	−0.2520	−0.0528
150	−1.4278	−1.2526	−1.0775	−0.9024	−0.7272	−0.5521	−0.3770	−0.2019	−0.0267	0.1484	0.3235
175	−0.8796	−0.7258	−0.5721	−0.4183	−0.2646	−0.1108	0.0429	0.1967	0.3505	0.5042	0.6580
175	−0.3924	−0.2386	−0.0849	0.0689	0.2226	0.3764	0.5301	0.6839	0.8376	0.9914	1.1451
200	0.0746	0.2093	0.3439	0.4786	0.6132	0.7478	0.8825	1.0171	1.1518	1.2864	1.4210
225	0.5004	0.6179	0.7353	0.8528	0.9702	1.0877	1.2051	1.3226	1.4400	1.5575	1.6749
250	0.8951	0.9971	1.0990	1.2009	1.3028	1.4047	1.5066	1.6085	1.7104	1.8123	1.9142
275	1.2663	1.3542	1.4420	1.5298	1.6175	1.7053	1.7931	1.8808	1.9686	2.0564	2.1441
300	1.6139	1.6890	1.7639	1.8388	1.9137	1.9885	2.0634	2.1383	2.2131	2.2880	2.3629
325	1.9215	1.9849	2.0480	2.1110	2.1741	2.2371	2.3002	2.3633	2.4263	2.4894	2.5524
350	2.1348	2.1875	2.2397	2.2919	2.3441	2.3963	2.4485	2.5007	2.5529	2.6051	2.6573

P = 1 bar for T < 100 °C; $P = P_{sat}$ for T ≥ 100 °C. Calculations performed using SUPCRT92 considering the thermodynamic data of minerals of Helgeson et al. (1978)

Table 7.2 Logarithm of the thermodynamic equilibrium constant of reaction (7.2), for pure clinochlore, muscovite, adularia, low-albite, and chalcedony (for T < 175 °C) or quartz/chalcedony (for T > 175 °C), log $K_{Na–Mg}$, as a function of the temperature and the ordering parameter Z of adularia

T(°C)	Z = 1	Z = 0.9	Z = 0.8	Z = 0.7	Z = 0.6	Z = 0.5	Z = 0.4	Z = 0.3	Z = 0.2	Z = 0.1	Z = 0
0.01	0.0139	0.1241	0.2342	0.3444	0.4545	0.5647	0.6748	0.7850	0.8951	1.0053	1.1154
25	0.4492	0.5452	0.6411	0.7370	0.8330	0.9289	1.0248	1.1208	1.2167	1.3127	1.4086
50	0.8219	0.9058	0.9897	1.0736	1.1575	1.2414	1.3254	1.4093	1.4932	1.5771	1.6610
75	1.1469	1.2205	1.2942	1.3678	1.4414	1.5150	1.5886	1.6623	1.7359	1.8095	1.8831
100	1.4360	1.5007	1.5654	1.6301	1.6948	1.7595	1.8242	1.8889	1.9536	2.0183	2.0830
125	1.6981	1.7550	1.8119	1.8689	1.9258	1.9827	2.0396	2.0965	2.1534	2.2103	2.2672
150	1.9400	1.9901	2.0401	2.0901	2.1402	2.1902	2.2403	2.2903	2.3403	2.3904	2.4404
175	2.1669	2.2108	2.2547	2.2987	2.3426	2.3865	2.4304	2.4744	2.5183	2.5622	2.6062
175	2.6540	2.6980	2.7419	2.7858	2.8298	2.8737	2.9176	2.9615	3.0055	3.0494	3.0933
200	2.8438	2.8823	2.9208	2.9593	2.9977	3.0362	3.0747	3.1131	3.1516	3.1901	3.2285
225	3.0286	3.0622	3.0957	3.1293	3.1628	3.1964	3.2300	3.2635	3.2971	3.3306	3.3642
250	3.2117	3.2408	3.2699	3.2990	3.3282	3.3573	3.3864	3.4155	3.4446	3.4737	3.5028
275	3.3950	3.4201	3.4452	3.4702	3.4953	3.5204	3.5455	3.5705	3.5956	3.6207	3.6458
300	3.5743	3.5957	3.6171	3.6385	3.6599	3.6813	3.7027	3.7241	3.7455	3.7669	3.7883
325	3.7313	3.7495	3.7675	3.7855	3.8035	3.8215	3.8395	3.8576	3.8756	3.8936	3.9116
350	3.8123	3.8274	3.8423	3.8572	3.8721	3.8871	3.9020	3.9169	3.9318	3.9467	3.9616

P = 1 bar for T < 100 °C; $P = P_{sat}$ for T ≥ 100 °C. Calculations performed using SUPCRT92 considering the thermodynamic data of minerals of Helgeson et al. (1978)

Equation (7.9) is valid from 0 to 175 °C, whereas Eq. (7.10) applies from 175 to 325 °C.

7.2 The $(K^+)^2/Mg^{2+}$ and $(Na^+)^2/Mg^{2+}$ Log Activity Ratios of the Selected Reservoir Liquids

The K^2/Mg log-activity ratios given by Eqs. (7.7) and (7.8) are shown in the diagrams of Figs. 7.1, 7.2, and 7.3, whereas the Na^2/Mg log-activity ratios given by Eqs. (7.9) and (7.10) are displayed in the graphs of Figs. 7.4, 7.5, and 7.6. In all these plots, the K^2/Mg and Na^2/Mg log-activity ratios are represented as a function of the absolute temperature inverse, from 100 to 350 °C, for the average log MAP value of −0.399 and for different values of the ordering parameter of adularia, namely Z = 1 (i.e., maximum-microcline), Z = 0 (i.e., high-sanidine), as well as Z = 0.559, Z = 0.820, and Z = 0.298, corresponding to the average value, the average value +1σ, and the average value −1σ, respectively, of the hydrothermal adularia in hypothetical equilibrium with the considered geothermal liquids (see Sect. 6.3). In all these diagrams are also displayed the K^2/Mg and Na^2/Mg log-activity ratios, as a function of 1/T(K), for both log MAP of −0.674, Z = 0 and log MAP of −0.270, Z = 1, to bracket most compositional variations of hydrothermal chlorites and illites. These theoretical K^2/Mg and Na^2/Mg log-activity ratios suggest that:

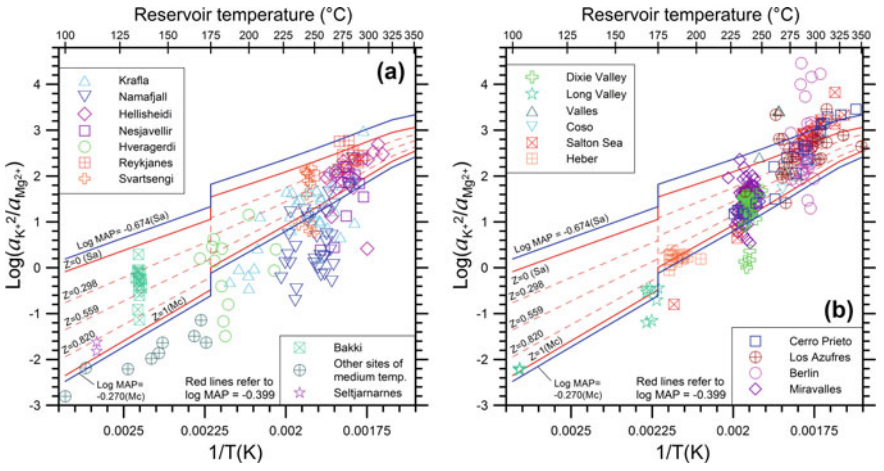

Fig. 7.1 K^2/Mg-log activity ratios of the selected reservoir liquids from the geothermal systems of **a** Iceland and **b** North-Central America as a function of aquifer temperature. Also shown are the K^2/Mg-log activity ratios fixed by equilibrium coexistence of clinochlore, muscovite, either chalcedony (below 175 °C) or quartz/chalcedony (above 175 °C), and adularia with ordering parameter Z = 1 and 0 (red solid lines), Z = 0.820, 0.559, and 0.298 (red dashed lines), all for log MAP = −0.399, as well as for log MAP = −0.674 and Z = 0 and for log MAP = −0.270 and Z = 1 (blue solid lines)

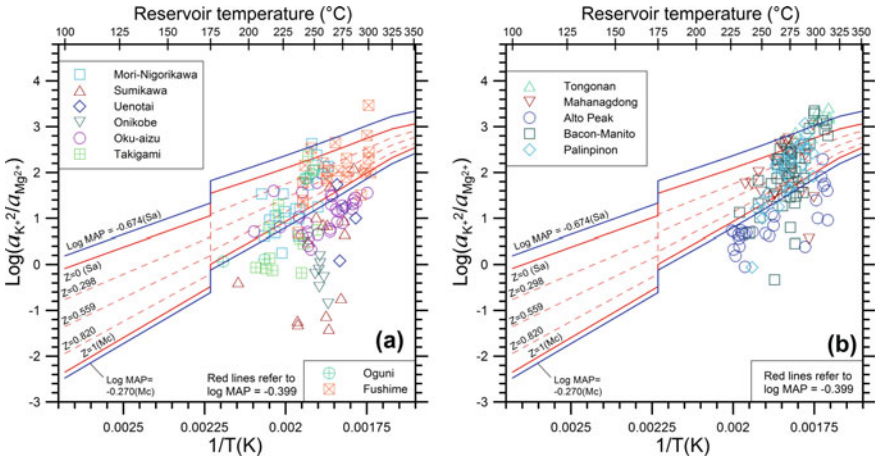

Fig. 7.2 K^2/Mg-log activity ratios of the selected reservoir liquids from the geothermal systems of **a** Japan and **b** The Philippines as a function of aquifer temperature. Also shown are the K^2/Mg-log activity ratios fixed by equilibrium coexistence of clinochlore, muscovite, either chalcedony (below 175 °C) or quartz/chalcedony (above 175 °C), and adularia with ordering parameter Z = 1 and 0 (red solid lines), Z = 0.820, 0.559, and 0.298 (red dashed lines), all for log MAP = −0.399, as well as for log MAP = −0.674 and Z = 0 and for log MAP = −0.270 and Z = 1 (blue solid lines)

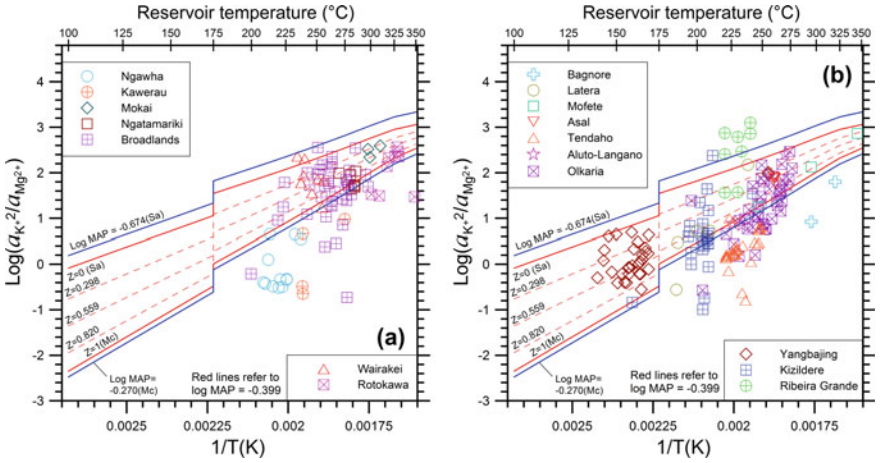

Fig. 7.3 K^2/Mg-log activity ratios of the selected reservoir liquids from the geothermal systems of **a** New Zealand and **b** miscellaneous sites as a function of aquifer temperature. Also shown are the K^2/Mg-log activity ratios fixed by equilibrium coexistence of clinochlore, muscovite, either chalcedony (below 175 °C) or quartz/chalcedony (above 175 °C), and adularia with ordering parameter Z = 1 and 0 (red solid lines), Z = 0.820, 0.559, and 0.298 (red dashed lines), all for log MAP = −0.399, as well as for log MAP = −0.674 and Z = 0 and for log MAP = −0.270 and Z = 1 (blue solid lines)

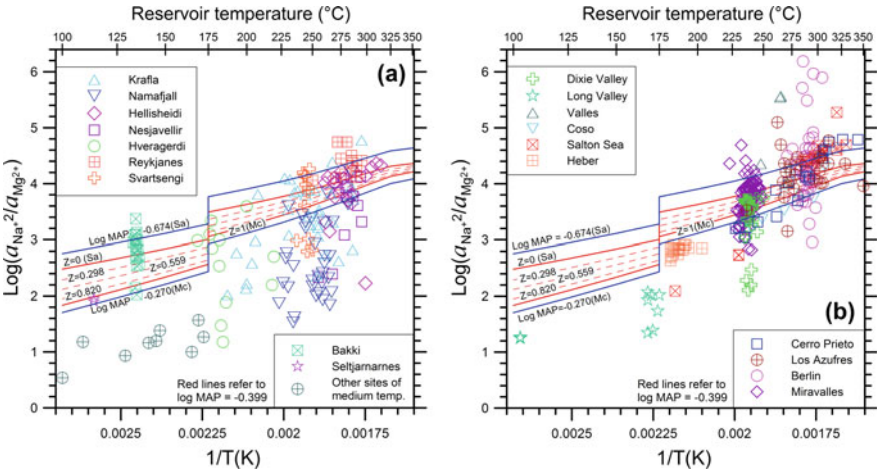

Fig. 7.4 Na^2/Mg-log activity ratios of the selected reservoir liquids from the geothermal systems of **a** Iceland and **b** North-Central America as a function of aquifer temperature. Also shown are the Na^2/Mg-log activity ratios fixed by equilibrium coexistence of clinochlore, muscovite, either chalcedony (below 175 °C) or quartz/chalcedony (above 175 °C), albite, and adularia with ordering parameter Z = 1 and 0 (red solid lines), Z = 0.820, 0.559, and 0.298 (red dashed lines), all for log MAP = −0.399, as well as for log MAP = −0.674 and Z = 0 and for log MAP = −0.270 and Z = 1 (blue solid lines)

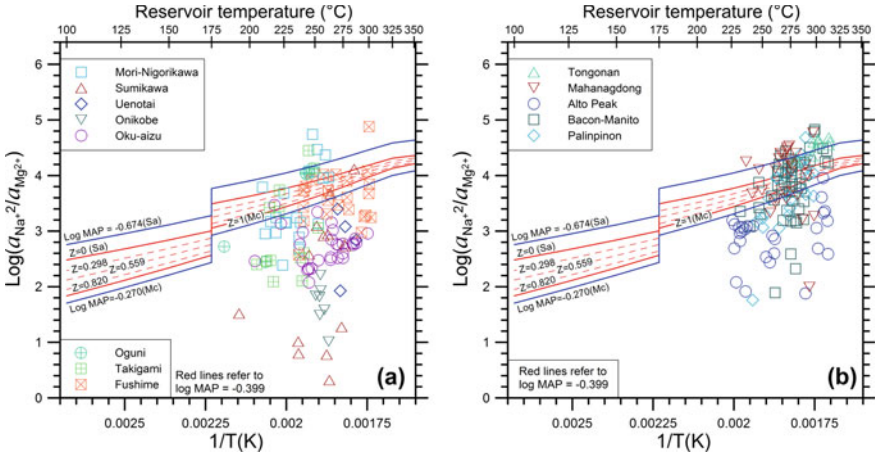

Fig. 7.5 Na^2/Mg-log activity ratios of the selected reservoir liquids from the geothermal systems of **a** Japan and **b** The Philippines as a function of aquifer temperature. Also shown are the Na^2/Mg-log activity ratios fixed by equilibrium coexistence of clinochlore, muscovite, either chalcedony (below 175 °C) or quartz/chalcedony (above 175 °C), albite, and adularia with ordering parameter Z = 1 and 0 (red solid lines), Z = 0.820, 0.559, and 0.298 (red dashed lines), all for log MAP = −0.399, as well as for log MAP = −0.674 and Z = 0 and for log MAP = −0.270 and Z = 1 (blue solid lines)

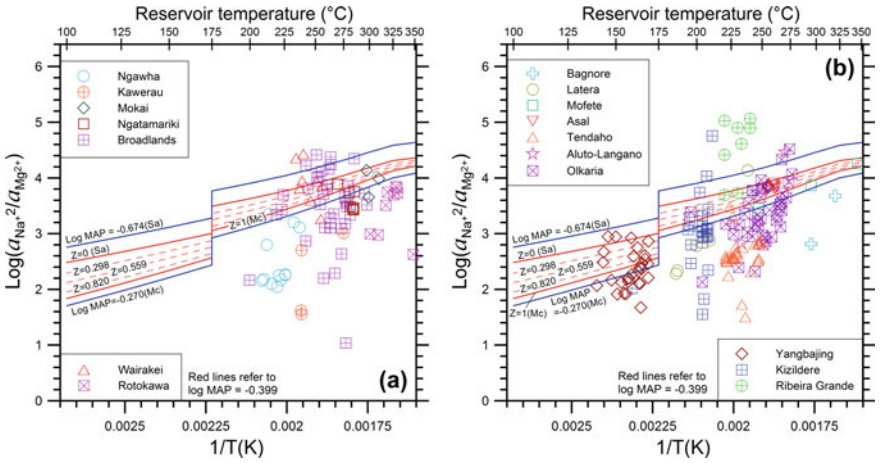

Fig. 7.6 Na^2/Mg-log activity ratios of the selected reservoir liquids from the geothermal systems of **a** New Zealand and **b** miscellaneous sites as a function of aquifer temperature. Also shown are the Na^2/Mg-log activity ratios fixed by equilibrium coexistence of clinochlore, muscovite, either chalcedony (below 175 °C) or quartz/chalcedony (above 175 °C), albite, and adularia with ordering parameter Z = 1 and 0 (red solid lines), Z = 0.820, 0.559, and 0.298 (red dashed lines), all for log MAP = −0.399, as well as for log MAP = −0.674 and Z = 0 and for log MAP = −0.270 and Z = 1 (blue solid lines)

1. The impact of the adularia order-disorder is more important on the K^2/Mg log-activity ratio than on the Na^2/Mg log-activity ratio. This fact is not surprising due to the distinct stoichiometric coefficients of adularia, 2.8 and 0.8, in reactions (7.1) and (7.2) controlling the K^2/Mg and Na^2/Mg log-activity ratios, respectively.
2. The effect of adularia order-disorder on the K^2/Mg log-activity ratio is slightly lower than that caused by the compositional changes of hydrothermal chlorites and illites, considering a range of $\pm 1\sigma$ around the mean a_{Clc} and a_{Ms} values. In contrast, the influence of adularia order-disorder on the Na^2/Mg log-activity ratio is appreciably lower than that brought about by the chemical variations of hydrothermal illites and chlorites, referring again to an interval of $\pm 1\sigma$ around the average a_{Clc} and a_{Ms} values. Also this fact is not surprising because adularia has different stoichiometric coefficients in reactions (7.1) and (7.2) whereas the stoichiometric coefficient of clinochlore is the same in both reactions and the same applies to muscovite.

Also shown in Figs. 7.1, 7.2, and 7.3 and in Figs. 7.4, 7.5, and 7.6 are the K^2/Mg- and Na^2/Mg-log activity ratios, respectively, of the selected geothermal liquids against the reciprocal of their aquifer temperatures (in K). Several reservoir liquids have K^2/Mg- and Na^2/Mg-log activity ratios within the range expected based on the different chemistry of hydrothermal chlorites and illites and the varying ordering parameter of adularia. Nevertheless, many reservoir liquids have K^2/Mg- and especially Na^2/Mg-log activity ratios lower than theoretical values. The Mg

concentration of these geothermal liquids is probably not representative of mineral-solution equilibrium due to presence of excess magnesium which is ascribable to different causes, as already pointed out in Sect. 5.6.2, including: (i) addition of Mg-rich fluids either external to the geothermal system or proceeding from shallower and colder parts of the geothermal system itself and (ii) cooling of the reservoir liquids and Mg acquisition, for instance during their travel from the upflow zone towards the outflow zone or due to breakthrough of re-injected brines (e.g., Fournier 1991). A few reservoir liquids have K^2/Mg- and especially Na^2/Mg-log activity ratios higher than theoretical values, possibly due to incorporation of Mg in the lattice of precipitating calcite or other solid phases, as already underscored in Sect. 5.6.2.

7.3 The Log MAP Values of the Selected Reservoir Liquids and Related Implications

The binary diagrams of Figs. 7.1, 7.2, 7.3, 7.4, 7.5, and 7.6 allows a comparison between the theoretical K^2/Mg- and Na^2/Mg-log activity ratios controlled by reactions (7.1) and (7.2) and the corresponding ratios of all the selected geothermal liquids in a single view. However, these binary diagrams do not allow a precise assessment of the consistency or inconsistency between theoretical and observed values for each aqueous solution. To gain more information on this subject, the log MAP values of the 973 geothermal liquids with Mg concentration higher than detection limit were computed and processed as described below.

First, the log $K_{K–Mg}$ and log $K_{Na–Mg}$ values were obtained for each geothermal liquid by inserting the reservoir temperature and the ordering parameter Z of adularia apparently in equilibrium with it into Eqs. (7.7) or (7.8) and Eqs. (7.9) or (7.10), respectively. The Z values >1 were assumed equal to one, whereas the Z values <0 were set to zero. Second, knowing the log $K_{K–Mg}$ and log $K_{Na–Mg}$ values as well as the K^2/Mg- and Na^2/Mg-log activity ratios of each aqueous solution, their log MAP values were computed by means of Eqs. (7.5) and (7.6), respectively. For each geothermal liquid, the log MAP values given by Eqs. (7.5) and (7.6) agree within less than 0.01 log-units[1]. Among the 973 reservoir liquids with Mg concentration higher than detection limit, 587 (60% of the cases) have negative log MAP values, ranging from −0.000639 to −2.59, while 386 (40% of the entries) have positive MAP values, varying from +0.00233 to +3.18.

The log MAP values computed from the K^2/Mg-log activity ratios are contrasted with these activity ratios in the binary diagrams of Figs. 7.7, 7.8, and 7.9, whereas the log MAP values calculated on the basis of the Na^2/Mg-log activity ratios are not considered to avoid unnecessary repetitions. In the diagrams of Figs. 7.7, 7.8, and 7.9, the reservoir liquids of a given geothermal system are distributed close or relatively

[1]These negligible differences are due to the approximations in the calculations of the ordering parameter Z of adularia by means of Eq. (6.2), log $K_{K–Mg}$ by using Eqs. (7.7) or (7.8), and log $K_{Na–Mg}$ by utilizing Eqs. (7.9) or (7.10).

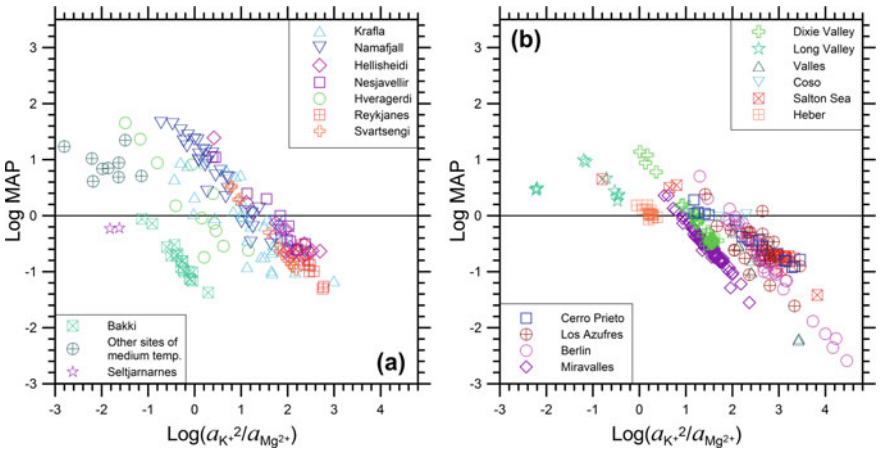

Fig. 7.7 Correlation diagrams between the log MAP values and K^2/Mg-log activity ratio for the selected reservoir liquids from the geothermal systems of **a** Iceland and **b** North-Central America

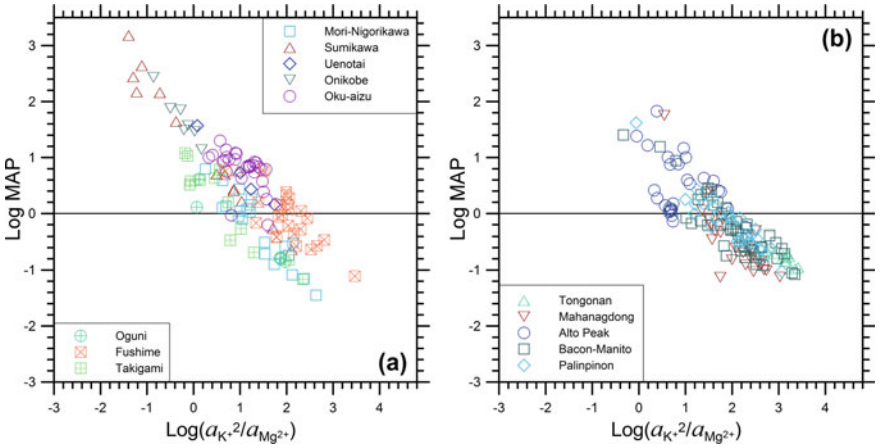

Fig. 7.8 Correlation diagrams between the log MAP values and K^2/Mg-log activity ratio for the selected reservoir liquids from the geothermal systems of **a** Japan and **b** The Philippines

close to a straight line of slope −1 and intercept depending on the aquifer temperature and the order/disorder degree of adularia. Tight trends are observed for the reservoir liquids of geothermal systems with little variations in both aquifer temperature and ordering parameter of adularia, as those coming from Bakki (Fig. 7.7a), Miravalles and Dixie Valley (Fig. 7.7b), and the shallow reservoir of Yangbajing (Fig. 7.9b). In contrast, the reservoir liquids of geothermal systems with significant changes in both aquifer temperature and ordering parameter of adularia, as is the case of Los Azufres (Fig. 7.7b), Fushime and Oku-aizu (Fig. 7.8a), Alto Peak (Fig. 7.8b), Broadlands (Fig. 7.9a) exhibit a considerable spread of data points. It should not be forgotten,

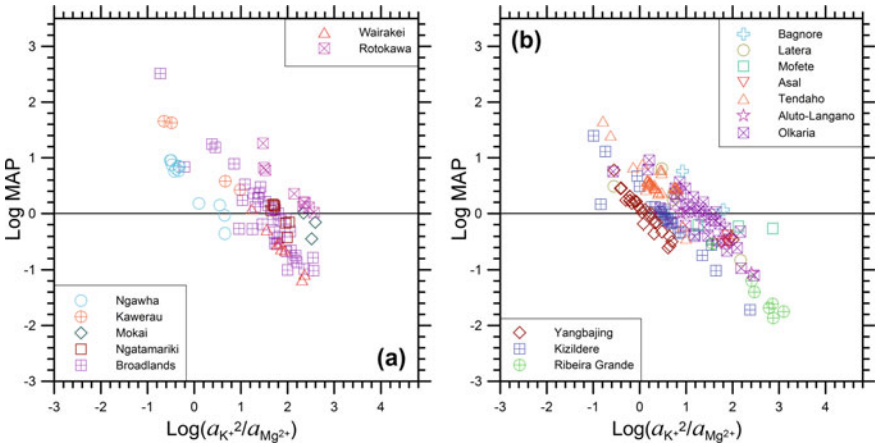

Fig. 7.9 Correlation diagrams between the log MAP values and K^2/Mg-log activity ratio for the selected reservoir liquids from the geothermal systems of **a** New Zealand and **b** miscellaneous sites

however, that the relation between log MAP values and K^2/Mg-log activity ratios may be influenced also by the number of samples available for each geothermal system.

Recalling that MAP is equal to $a_{Clc}^{0.2} \cdot a_{Ms}^{0.8}$ and that both a_{Clc} and a_{Ms} cannot be higher than one, it follows that the maximum permissible value of log MAP is zero for an aqueous solution in equilibrium with the hydrothermal minerals involved in reactions (7.1) and (7.2). Consequently, only the geothermal liquids with negative log MAP values may be representative of reservoir conditions, although possible effects of Mg loss cannot be excluded as already underscored above and in Sect. 5.6.2. In contrast, the geothermal liquids with positive log MAP values are certainly affected by presence of excess (non-equilibrium) Mg, for the reasons given above and in Sect. 5.6.2.

Minimum muscovite activities of the illites in apparent equilibrium with the 587 reservoir liquids with negative log MAP values were computed for $a_{Clc} = 1$ and minimum clinochlore activities of the chlorites in apparent equilibrium with these aqueous solutions were calculated for $a_{Ms} = 1$. Computed minimum values of muscovite activity range between 5.79×10^{-4} and 0.998, with a mean of 0.292, a median of 0.209 and a standard deviation of 0.248. Calculated minimum values of clinochlore activity distribute in a much wider interval, from 1.13×10^{-13} to 0.991, with an average of 0.0720, a median of 0.00191 and a standard deviation of 0.0720. These computed minimum values of a_{Ms} and a_{Clc} partly overlap the ranges of muscovite and clinochlore activities of the hydrothermal illites and chlorites (see Sect. 7.1).

Furthermore, computed minimum values of a_{Ms} and a_{Clc} could be used to speculate, to some extent, on both the lithology of reservoir rocks and the possible seawater recharge, as already recalled in Sect. 4.4.2. In fact, on the one hand, chlorite chemistry depends upon the composition of both reservoir rock and other hydrothermal

minerals (e.g., Albee 1962; De Caritat et al. 1993). On the other hand, the composition of chlorites can be controlled by fluid chemistry, at least in part. For instance, the Mg-rich chlorites of Reykjanes and Bouillante might be due to the inflow of Mg-rich seawater into these geothermal systems, as recognized by Arnórsson (1978a) for Reykjanes and Sanjuan et al. (2001) for Bouillante. Nevertheless, the computed minimum values of a_{Ms} and a_{Clc} have limited importance for practical purposes.

Let us now consider the 386 geothermal liquids with positive MAP values. For these geothermal liquids, it is possible to compute the maximum molality of free Mg^{2+} ion fixed by equilibrium with the hydrothermal minerals participating to reactions (7.1) and (7.2), through the following two relations:

$$\log m_{Mg^{2+},max.eq} = 2 \cdot \log a_{K^+} - \log \gamma_{Mg^{2+}} - \log K_{K-Mg} \tag{7.11}$$

$$\log m_{Mg^{2+},max.eq} = 2 \cdot \log a_{Na^+} - \log \gamma_{Mg^{2+}} - \log K_{Na-Mg} \tag{7.12}$$

which are obtained rearranging Eqs. (7.5) and (7.6) and assuming unit values for both a_{Ms} and a_{Clc}. Activities of muscovite and clinochlore <1 would lead to lower molalities of free Mg^{2+} ion. For the reservoir liquids with $0 \leq Z \leq 1$, the $m_{Mg^{2+},max.eq}$ given by Eq. (7.11) matches closely the $m_{Mg^{2+},max.eq}$ obtained by Eq. (7.12), with an average deviation of 0.16 ± 0.25 (1σ) %. For the reservoir liquids with $Z > 1$ or $Z < 0$, the adularia ordering parameter was set to 1 and 0, respectively, leading to higher discrepancies between the two $m_{Mg^{2+},max.eq}$ values computed by means of Eqs. (7.11) and (7.12).

For the 386 geothermal liquids with positive MAP values, the maximum molality of free Mg^{2+} ion, computed for mineral-solution equilibrium and $a_{Ms} = a_{Clc} = 1$ is contrasted with the analytical molality of free Mg^{2+} ion in the correlation plots of Figs. 7.10, 7.11, and 7.12. The shifts to the right of the equality line allow one to evaluate the minimum concentration of excess (non-equilibrium) Mg present in each reservoir liquid. In turn, these data can be used to recognize and quantify the processes controlling excess Mg, such as cooling and mixing (see above). To be recalled that mixing of Mg-rich, low-temperature waters from shallow levels with SiO_2-rich, high temperature waters from deep levels may lead to smectite scaling as recognized at Tongonan, Palinpinon, and Bacon-Manito in The Philippines (Reyes and Cardile 1989), in several geothermal district heating systems in Iceland (Gunnlaugsson and Einarsson 1989; Kristmannsdóttir et al. 1989; Hauksson et al. 1995), at Onikobe, Japan (Ajima et al. 1998), and in the Mori geothermal power plant (Kasai et al. 2000). Cooling by boiling was instead invoked to explain smectite scaling in the surface facilities of the Mindanao geothermal field (Dulce et al. 2010).

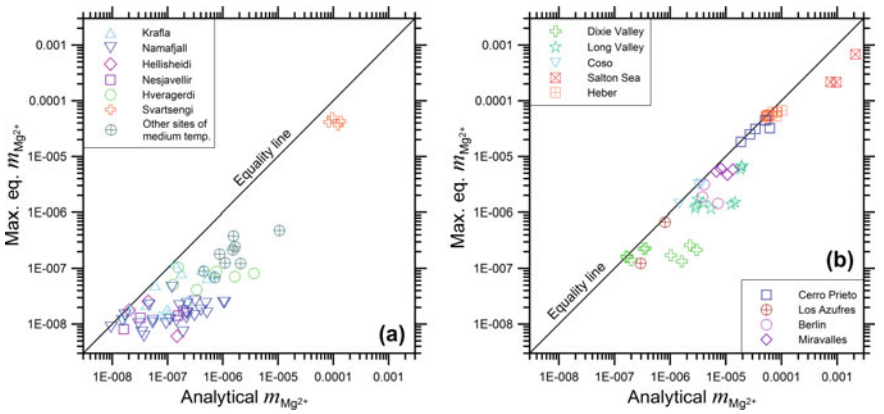

Fig. 7.10 Correlation plot between the maximum equilibrium molality of free Mg^{2+} ion and the analytical molality of free Mg^{2+} ion for the selected reservoir liquids with positive MAP values from the geothermal systems of **a** Iceland and **b** North-Central America

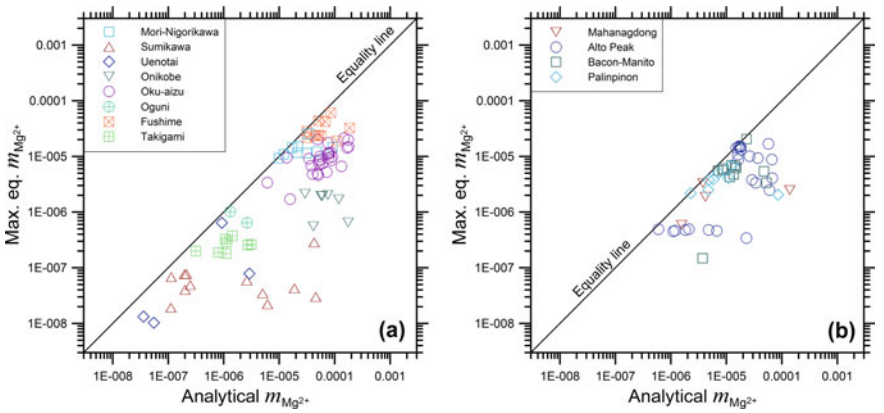

Fig. 7.11 Correlation plot between the maximum equilibrium molality of free Mg^{2+} ion and the analytical molality of free Mg^{2+} ion for the selected reservoir liquids with positive MAP values from the geothermal systems of **a** Japan and **b** The Philippines

7.4 Final Considerations on the Use of the K^2/Mg- and Na^2/Mg-Activity Ratios

Summing up, the K^2/Mg- and Na^2/Mg-activity ratios of reservoir liquids are controlled by the aquifer temperature, the order-disorder degree of hydrothermal adularia, and the mineral activity product $\mathrm{MAP} = a_{\mathrm{Clc}}^{0.2} \cdot a_{\mathrm{Ms}}^{0.8}$, involving the activity of clinochlore in hydrothermal chlorite and the activity of muscovite in hydrothermal illite.

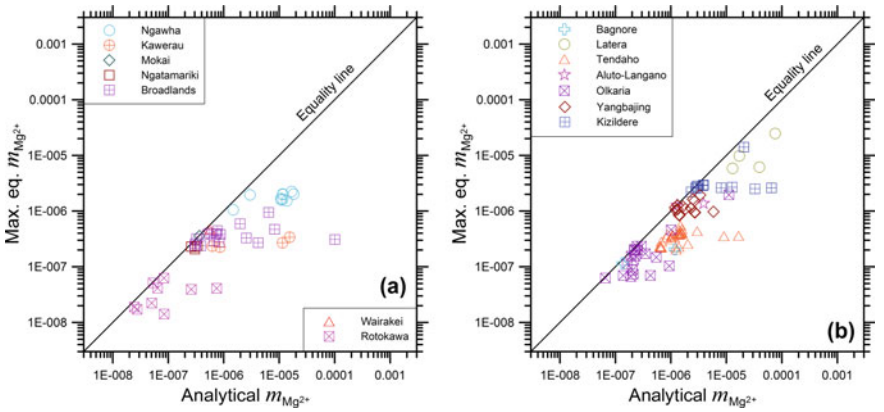

Fig. 7.12 Correlation plot between the maximum equilibrium molality of free Mg^{2+} ion and the analytical molality of free Mg^{2+} ion for the selected reservoir liquids with positive MAP values from the geothermal systems of **a** New Zealand and **b** miscellaneous sites

For the reservoir liquids with negative MAP values, the K^2/Mg- and Na^2/Mg-activity ratios can be used to obtain information on the minimum activities of clinochlore in chlorites and of muscovite in illites, which are in apparent equilibrium with the aqueous solutions of interest. For the reservoir liquids with positive MAP values, the K^2/Mg- and Na^2/Mg-activity ratios can be utilized to assess the minimum concentrations of excess (non-equilibrium) Mg and, consequently, to identify and quantify the processes controlling excess Mg, such as cooling and mixing, which may lead to Mg-silicate (e.g., smectite) scaling. This is probably the most valuable information provided by the activity-based theoretical K–Mg and Na–Mg geoindicators.

The K–Mg and Na–Mg exchange reactions other than (7.1) and (7.2), discussed in Sect. 5.6.3, are not explored here to develop alternative K–Mg and Na–Mg geoindicators for two main reasons, namely the restricted temperature range in which they are expected to be effective and the limitations caused by the varying characteristics of the relevant Mg-bearing minerals. For what concerns the first reason, the exchange reactions involving phlogopite, diopside, tremolite, and talc should work above ~280 °C, whereas the exchange reactions including Mg-montmorillonite and dolomite should be active below ~180 °C (e.g., Henley and Ellis 1983; Reyes 1990). For what concerns the second reason, phlogopite is a component of biotite, diopside is a component of clinopyroxene, tremolite is a component of amphibole, and Mg-montmorillonite is a component of smectites, whereas the thermodynamic properties of dolomite are strongly influenced by order-disorder. Therefore, alternative K–Mg and Na–Mg geoindicators are expected to be affected by limitations similar to or even worse than those of the K–Mg and Na–Mg geoindicators derived above for the exchange reactions involving clinochlore as Mg-bearing solid phase.

References

Ajima S, Todaka N, Murakake H (1998) An interpretation of smectite precipitation in production wells caused by the mixing of different geothermal fluids. In: Proceedings of 23rd Workshop on Geothermal Reservoir Engineering. Stanford University, pp 264–269

Albee AL (1962) Relationships between the mineral association, chemical composition and physical properties of the chlorite series. Am Mineral 47:851–870

Arnórsson S (1978) Major element chemistry of the geothermal sea-water at Reykjanes and Svartsengi. Iceland Mineral Mag 42:209–220

De Caritat P, Hutcheon I, Walshe JL (1993) Chlorite geothermometry: a review. Clay Clay Miner 41:219–239

Dulce RG, Aragon GM, Sambrano BG, Bayrante LF (2010) Genesis of smectite scales in Mindanao geothermal production field, Philippines. In: Proceedings World Geothermal Congress. Bali, Indonesia, p 9

Fournier RO (1991) Water geothermometers applied to geothermal energy. In: Application of Geochemistry in Geothermal Reservoir Development. F. D'Amore, co-ordinator, UNITAR, pp 37–69

Giggenbach WF (1988) Geothermal solute equilibria. derivation of Na–K–Mg–Ca geoindicators. Geochim Cosmochim Ac 52:2749–2765

Gunnlaugsson E, Einarsson A (1989) Magnesium-silicate scaling in mixture of geothermal water and deaerated fresh water in a district heating system. Geothermics 18:113–120

Hauksson T, Pórhallsson S, Gunnlaugsson E, Albertsson A (1995) Control of magnesium silicate scaling in district heating systems. World Geotherm Congr, Florence, Italy, pp 18–31

Helgeson HC, Delany JM, Nesbitt HW, Bird DK (1978) Summary and critique of the thermodynamic properties of rock-forming minerals. Am J Sci 278A:229

Henley RW, Ellis AJ (1983) Geothermal systems ancient and modern: a geochemical review. Earth-Sci Rev 19:1–50

Kasai K, Sato K, Kimura SI, Shakunaga N, Obara K (2000) Characterization of smectite scale and scale inhibition test by pH control at the Mori geothermal power plant, Japan. Proc World Geothermal Congr 1331–1336

Kristmannsdóttir H, Ólafsson M, Thórhallsson S (1989) Magnesium silicate scaling in district heating systems in Iceland. Geothermics 18:191–198

Reyes AG (1990) Petrology of Philippine geothermal systems and the application of alteration mineralogy to their assessment. J Volcanol Geoth Res 43:279–309

Reyes AG, Cardile CM (1989) Characterization of clay scales forming in Philippine geothermal wells. Geothermics 18:429–446

Sanjuan B, Brach M, Lasne E (June, 2001) Bouillante geothermal fluid: mixing and water/rock interaction processes at 250 °C. In: Cidu R (ed.), Water-rock interaction, WRI-10, international symposium on water-rock interaction, vol 2. Villasimius, Italy. A.A. Balkema, pp 911–914